Experimental Investigations of Particulate Size and Number Distribution in an Ethanol and Methanol Fueled HCCI Engine

Article *in* Journal of Energy Resources Technology, Transactions of the ASME · July 2014

DOI: 10.1115/1.4027897

CITATIONS
45

READS
644

2 authors, including:

Avinash Kumar Agarwal
Indian Institute of Technology Kanpur
580 PUBLICATIONS **23,048** CITATIONS

SEE PROFILE

Experimental Investigations of Particulate Size and Number Distribution in an Ethanol and Methanol Fueled HCCI Engine

Rakesh Kumar Maurya[1]
Engine Research Laboratory,
Department of Mechanical Engineering,
Indian Institute of Technology Kanpur,
Kanpur 208016, India

Avinash Kumar Agarwal[2]
Engine Research Laboratory,
Department of Mechanical Engineering,
Indian Institute of Technology Kanpur,
Kanpur 208016, India
e-mail: akag@iitk.ac.in

Alcohols (ethanol and methanol) are being widely considered as alternative fuels for automotive applications. At the same time, homogeneous charge compression ignition (HCCI) engine has attracted global attention due to its potential of providing high engine efficiency and ultralow exhaust emissions. Environmental legislation is becoming increasingly stringent, sharply focusing on particulate matter (PM) emissions. Recent emission norms consider limiting PM number concentrations in addition to PM mass. Therefore, present study is conducted to experimentally investigate the effects of engine operating parameters on the PM size–number distribution in a HCCI engine fueled with gasoline, ethanol, and methanol. The experiments were conducted on a modified four-cylinder diesel engine, with one cylinder modified to operate in HCCI mode. Port fuel injection was used for preparing homogeneous charge in the HCCI cylinder. Intake air preheating was used to enable auto-ignition of fuel–air mixture. Engine exhaust particle sizer (EEPS) was used for measuring size–number distribution of soot particles emitted by the HCCI engine cylinder under varying engine operating conditions. Experiments were conducted at 1200 and 2400 rpm by varying intake air temperature and air–fuel ratio for gasoline, ethanol, and methanol. In this paper, the effect of engine operating parameters on PM size–number distribution, count mean diameter (CMD), and total PM numbers is investigated. The experimental data show that the PM number emissions from gasoline, ethanol, and methanol in HCCI cannot be neglected and particle numbers increase for relatively richer mixtures and higher intake air temperatures. [DOI: 10.1115/1.4027897]

Keywords: particle size-number distribution, HCCI, ethanol, methanol, gasoline

1 Introduction

Stringent emission legislations and harmful environmental impact of engine-out emissions create necessity to explore different combustion concepts for internal combustion engines. HCCI engine is an alternative combustion concept having potential for very high thermal efficiency and ultralow NO_x emissions. In HCCI combustion mode, the fuel–air mixture is homogeneously distributed in the combustion chamber, and there is no diffusion combustion with high temperature combustion zones [1]. In HCCI combustion, auto-ignition occurs simultaneously at several sites in the combustion chamber, leading to 3D heat release. To control the HCCI combustion heat release, highly diluted (by air or residual burned gas) charge is supplied to the cylinder. Major challenges in HCCI engine are to extend the operating window to increase high load limit and controlling the ignition timings. In HCCI engine, the ignition timing is primarily controlled by chemical kinetics and is therefore affected by fuel composition, equivalence ratio, and thermodynamic state of air–fuel mixture [2]. HCCI engines have higher HC and CO emissions compared to conventional diesel engines due to relatively lower in-cylinder temperatures caused by lean-burn, high-dilution combustion [3]. Lower in-cylinder temperature inside the combustion chamber results in incomplete combustion and reduction in postcombustion oxidation rates inside the cylinder.

HCCI engines are inherently fuel-flexible and can be operated using low- or high-grade fuels, given that the fuel–air mixture can be heated up to auto-ignition temperature of the fuel in the combustion chamber [4]. In particular, HCCI engines can be operated on primary alcohols such as ethanol and methanol [5–7]. Alcohols are attractive alternatives to gasoline/diesel, and they are identified as fuels having potential to improve urban air quality due to their cleaner combustion characteristics [8]. Alcohols, mainly ethanol and to a lesser extent methanol, are considered as alternative fuels for internal combustion engines [9–11]. Ethanol is a biomass-derived renewable fuel, which can be produced by fermentation of sugars from organic biomass materials [12]; however, methanol is mainly produced from coal- or petrol-based fuels and natural gas. All gasoline spark ignition (SI) engines can tolerate some fraction of ethanol blended in gasoline (~10%), and most of them can be readily converted to flexi-fuel engines to operate on fuels containing up to 85% ethanol [13]. It is important to fully understand ethanol combustion and emission characteristics in advanced combustion systems, such as HCCI. In a concurrent study, ethanol was recently characterized for HCCI operation over wide range of engine speeds, intake pressures, and loads [6,14]. Recently, HCCI combustion characteristics were also investigated for utilization of wet ethanol [15,16]. Some of these studies specifically focused on the emission characteristics of ethanol fueled HCCI engines [17]. All these studies conducted using ethanol and methanol on HCCI engine however did not focus on the PM emissions.

PM emitted in the engine exhaust has severe adverse effects on human health and the environment. Findings of numerous medical

[1]Present address: School of Mechanical, Materials and Energy Engineering, Indian Institute of Technology Ropar, Rupnagar 140001, India.
[2]Corresponding author.

Contributed by the Internal Combustion Engine Division of ASME for publication in the JOURNAL OF ENERGY RESOURCES TECHNOLOGY. Manuscript received August 9, 2013; final manuscript received June 19, 2014; published online July 29, 2014. Assoc. Editor: Timothy J. Jacobs.

Table 1 Unmodified test engine specifications

Make/Model	Mahindra/Loadking
No. of cylinders	Four
Displaced volume	652 cc/cylinder
Stroke/Bore	94/94 mm
Connecting rod length	158 mm
Compression ratio	17.5:1
Number of valves	2/cylinder
Exhaust valve open/close	56 deg BBDC/5 deg ATDC
Inlet valve open/close	10 deg BTDC/18 deg ABDC

investigations indicate that several health effects are associated with ultrafine particles having diameters below 100 nm, which are typically emitted during the combustion of fossil fuels. Researchers showed that fine particles can penetrate the cell membranes, enter into the blood stream, reach brain, and even have some mutagenic effects [18,19]. Therefore, measurement and control of engine PM emissions is absolutely necessary. Conventional gasoline SI engines are not known for emission of smoke or soot. However, several recent studies conducted to investigate gasoline PM emissions showed that particle emissions from gasoline engines are significant and comparable to diesel engines [20–23]. Parameters such as the air/fuel ratio, fuel injection timing, and engine load can increase PM emissions by as much as three orders of magnitude as compared to those for a stoichiometric operation in gasoline engines [20–22].

In HCCI engine, PM or smoke emissions are frequently reported as "near zero" or "ultralow" [24]. However, recent studies revealed that although the total PM mass is indeed low, significant numbers of these particles remain in the size range below 100 nm mobility diameter [25–30]. The study conducted for investigation of port fuel injection timing on methanol fueled HCCI combustion showed that particle number emissions are dependent on fuel injection timings and found that start of injection during closed intake valve condition have lower peak concentration of particles [7]. Price et al. investigated PM emissions from a gasoline fueled HCCI engine using DI-HCCI fueling strategy and found that nucleation mode had a significantly higher particle number concentration than the accumulation mode [26]. Franklin investigated the effect of different HCCI control strategies on the PM emissions [30]. Findings of this study strongly suggested that although essentially free of accumulation mode (soot) particles, nucleation mode particles are present in significant mass and numbers in the exhaust of fully premixed HCCI engines. Precursors to these particles are believed to primarily originate from more volatile species present in the lubricating oil. The abundance of volatile precursors and lack of adsorption and condensation sites create ideal conditions for homogeneous nucleation [30]. A recent study by Singh et al. on the characterization of exhaust particulates from diesel fueled HCCI engine revealed that PM emissions from the HCCI engines largely depend on EGR rate and relative air–fuel ratio (λ) [31].

All these factors mentioned above indicate that the thermal conditions prevailing in the combustion chamber and the fuel injection timing, at which a HCCI engine is operated, certainly has a direct influence on engine emissions, especially PM emissions. Therefore, in this study, the effect of engine operating conditions on particle number emissions from a port fuel injected HCCI engine using gasoline, ethanol, and methanol is investigated comprehensively.

2 Experimental Setup

In this section, a brief description of experimental setup is given. Experimental setup is described in detail in a previous research paper [7]. A naturally aspirated diesel engine (Loadking; Mahindra) was modified for achieving HCCI combustion in one of the four engine cylinder and conducting the present experimental study. Specifications of the unmodified engine are given in Table 1. The engine was coupled with an eddy current dynamometer (ECB200; Dynalec).

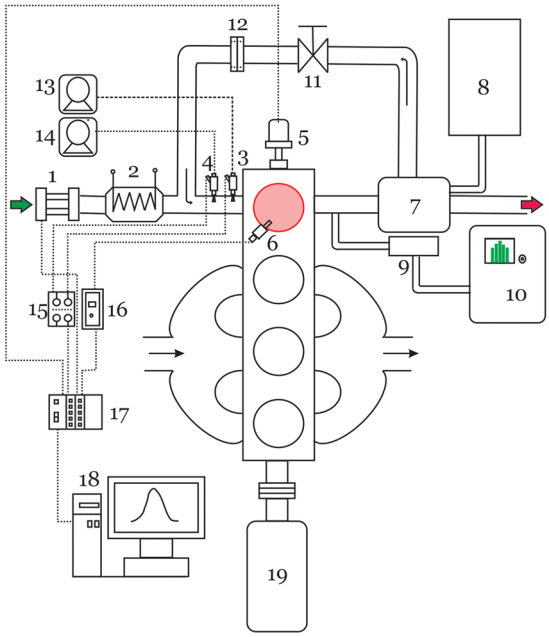

1. Hot-film Air Mass Meter 2. Air Preheater 3. Solenoid Fuel Injector 1
4. Solenoid Fuel Injector 2 5. Precision Shaft Encoder
6. Peizoelectric Pressure Transducer 7. Exhaust Plenum
8. Raw Exhaust Emission Analyzer 9. Thermo-diluter 10. EEPS
11. EGR Valve 12. Orifice Plate 13. Fuel Tank 1 with Fuel Pump
14. Fuel Tank 2 with Fuel Pump 15. Injector Driver Circuit
16. Charge Amplifier 17. Compact RIO 18. Data Logging Computer
19. Eddy Current Dynamometer

Fig. 1 Schematic of the experimental setup

Schematic of the experimental setup is shown in Fig. 1. A port fuel injector was installed in the intake manifold for premixed charge preparation in the HCCI cylinder. The fuel injection timing and duration were controlled by a microcontroller (cRIO-9014, National Instruments) and a customized injection driver circuit.

HCCI combustion phasing was controlled by intake air preheating. The intake air was preheated using an electric air preheater upstream of the intake manifold, which was controlled by a closed-loop controller, and a constant intake air temperature was maintained. The air mass flow rate in the HCCI cylinder was measured by a hot-film air mass flow meter. The in-cylinder pressure was measured using a piezo-electric pressure transducer mounted flush with the cylinder head. The in-cylinder pressure history data acquisition and combustion analysis were done using LabVIEW-based program, specifically developed for this study.

The particle size–number distribution in the exhaust gas was measured using (EEPS 3090, TSI). The EEPS spectrometer is a fast-response, high-resolution instrument, which measures particle number concentrations in the diluted engine exhaust. It measures particle sizes ranging from 5.6 to 560 nm with a size resolution of 16 channels per decade (a total of 32 channels). The instrument draws a sample of exhaust into the inlet continuously (Fig. 1). Rotating disk thermodiluter is required for diluting and preconditioning the exhaust gas before it is supplied to the EEPS (Fig. 1). A portion of raw exhaust is mixed with the preheated and prefiltered air in the disk cavity of the thermodiluter. The thermodiluter draws exhaust gas sample directly from the exhaust line using a sampling probe. The sampling probe is designed in such a manner that the particle losses due to nonisokinetic sampling are negligible. Exhaust gas sampling was done at a dilution ratio of 114:1 in the present investigations. The particle measurement was done at a steady-state engine operating condition when the intake air temperature, coolant temperature, cylinder head temperature, engine load, and speed values were stable. PM measurements were started after running the engine for 10 min under steady-state

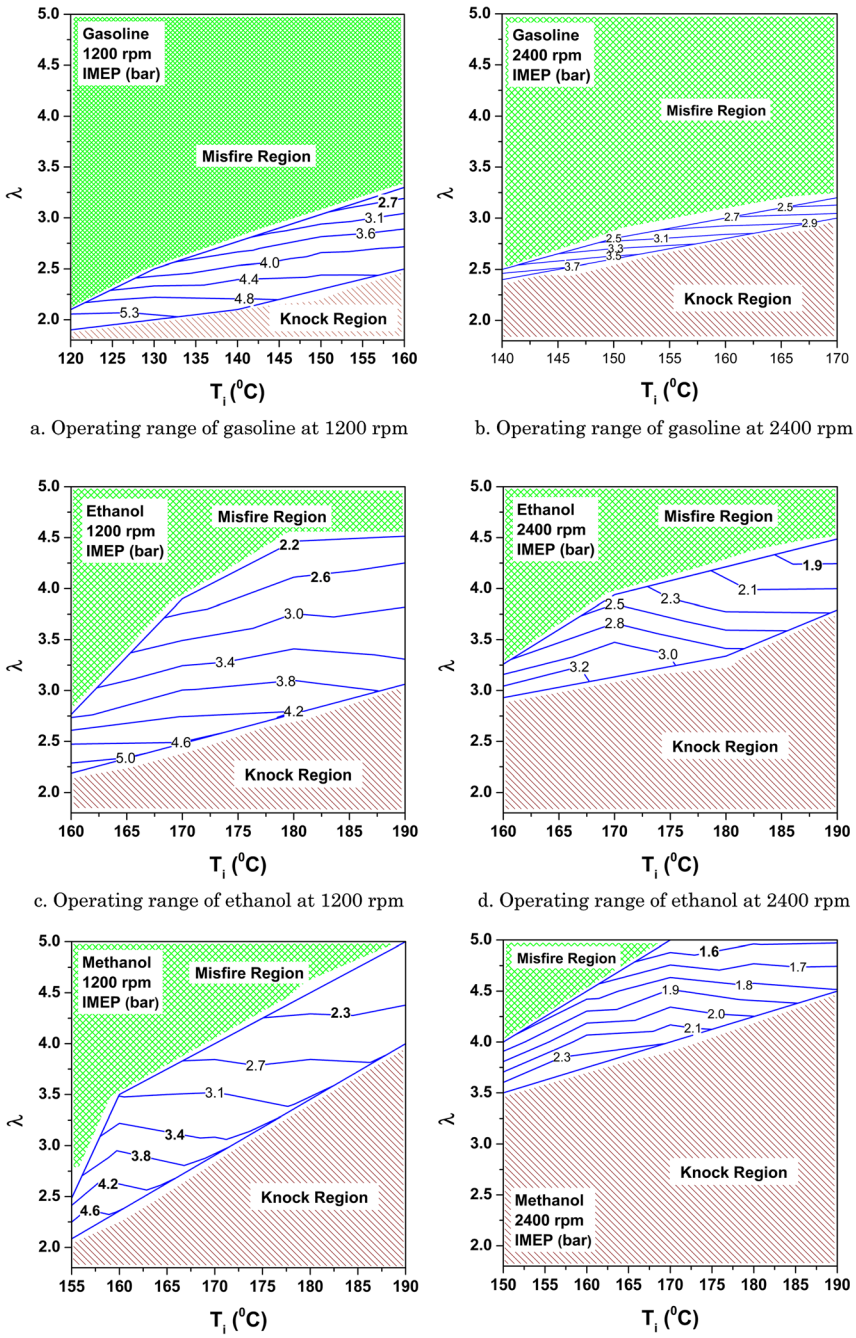

Fig. 2 HCCI operating range for gasoline, ethanol, and methanol

operating conditions. The particle number concentration data were acquired at a sampling frequency of 1 Hz. The particle number concentration presented in this investigation was an average of one minute data (i.e., 60 data points). The coefficient of variation (COV) of particle number concentration was calculated for each particle size for all the test conditions from the 60 measured data points. The maximum COV was 1.5% among all test conditions. Each test was repeated twice in order to ensure repeatability of the trends.

3 Results and Discussion

In this section, the experimental results of HCCI combustion generated PM emissions for different engine operating conditions are presented for gasoline, ethanol, and methanol. The results are presented for size–number distribution of PM per unit volume of engine exhaust (after accounting for the dilution factor). The experiments were conducted at different intake air temperatures and relative air–fuel ratios (λ) at two engine speed (1200 and 2400 rpm) using ethanol, methanol, and gasoline in HCCI combustion mode.

Figure 2 shows the HCCI operating range for gasoline, ethanol, and methanol, respectively. The HCCI operating range is determined by chalking out operating limits of high (knock limited) and low load boundaries (combustion stability limited). In this study, ringing intensity (RI) is used as a criterion to define the high load HCCI limit (knock boundary). COV of the indicated mean effective pressure (IMEP) is used as a criterion to define the low load HCCI limit, which a measure of combustion stability. COV_{IMEP} is calculated using data acquired for 2000 consecutive engine cycles and is used to define the low load HCCI limit (misfire boundary). In this study, acceptable higher and

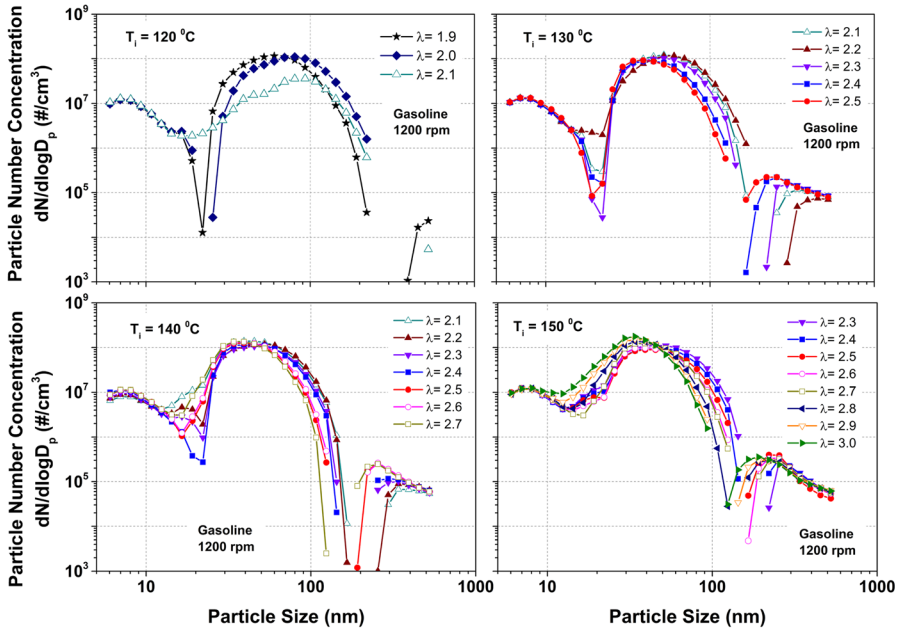

(a) Particle size distribution at 1200 rpm

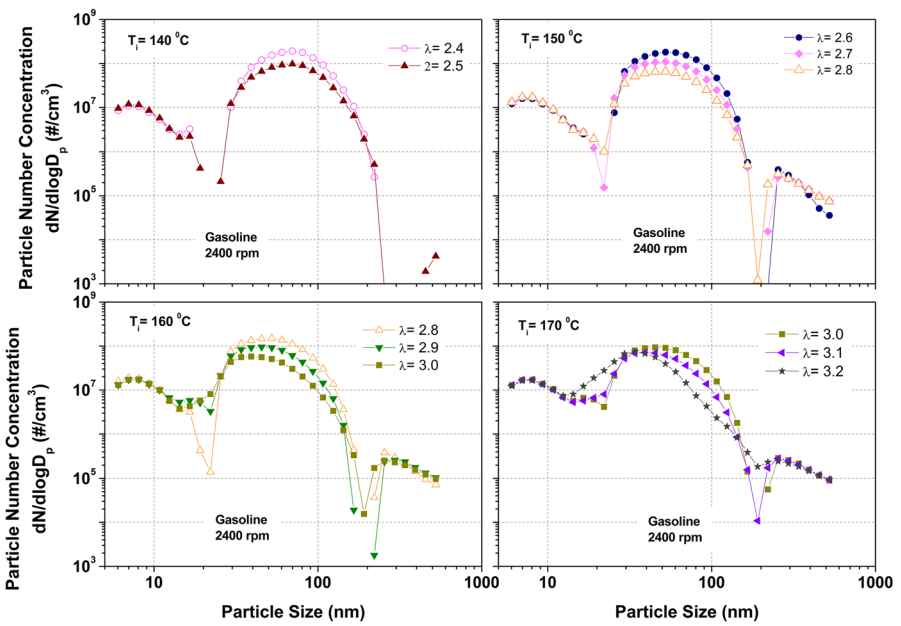

(b) Particle size distribution at 2400 rpm

Fig. 3 Particle size–number distributions for gasoline HCCI combustion with varying intake temperature and λ

lower boundary values are taken as $RI < 6\,MW/m^2$ and $COV_{IMEP} < 3.5\%$. These values are taken from the open literature for similar displacement engines [32,33]. Figure 2 shows HCCI operating range using above criterion of high and low load HCCI limits for gasoline, ethanol, and methanol at engine speeds of 1200 rpm and 2400 rpm. In Fig. 2, contour lines represent the constant IMEP lines. It can be observed from Fig. 2 that the IMEP contours are more horizontally inclined for all test fuels and speeds. This indicates that IMEP (contour lines) is mainly affected by the air–fuel ratio (λ) in the HCCI operating region. The intake air temperature mainly affects combustion phasing, which has a rather weak effect on IMEP in operating range defined by the high and low load HCCI limits for all test fuels. It is obvious that the engine output in the HCCI operating range is determined by the relative air/fuel ratio (λ) since richer mixtures (higher energy input) lead to higher power output. It can be noticed from Fig. 2 that IMEP decreases as the engine operates on leaner mixtures and IMEP increases as engine operates on richer mixtures and lower intake air temperatures.

It can also be observed from Fig. 2 that the area of operating region decreases with increasing engine speed for all test fuels. As the engine speed increases, minimum λ (richest mixture) in the HCCI operating range increases (i.e., mixture becomes leaner) for each fuel, which leads to lowering of higher load boundary due to lower energy input (i.e., leaner mixture). It can be noticed that for gasoline, higher intake air temperature is required at higher engine speeds, while ethanol does not require such elevated intake air temperatures. Therefore, the requirement of higher inlet air

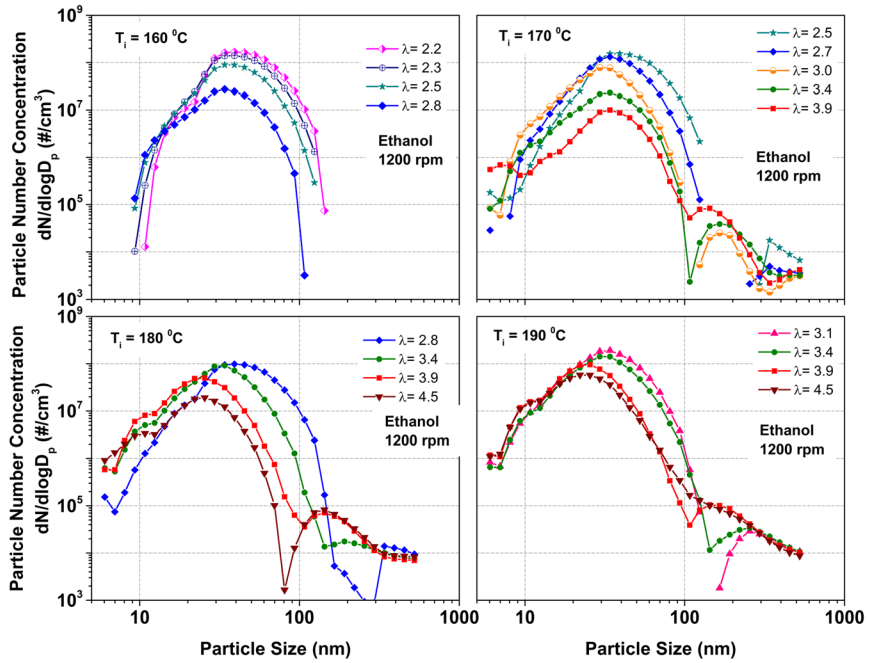

(a) Particle size distribution at 1200 rpm.

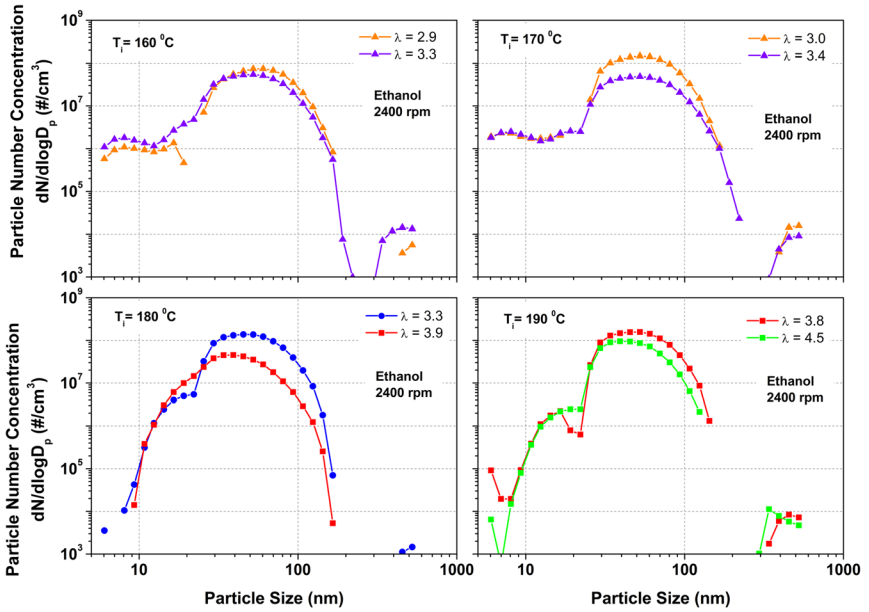

(b) Particle size distribution at 2400 rpm.

Fig. 4 Particle size–number distributions for ethanol HCCI combustion with varying intake temperature and λ

temperature at higher engine speeds is dependent on fuel properties. Higher intake air temperature is required for two reasons: First, there is less time for the chemical reactions to setoff the auto-ignition process at higher engine speeds, and second, due to small inlet valve diameter and pressure drop over the intake air heater, volumetric efficiency decreases with increased engine speeds. To compensate for this pressure drop, the intake air temperature has to be raised at higher engine speeds. However, higher engine speed reduces the heat transfer, which in-turn increases the temperature inside the combustion chamber. This is an opposing factor, which lowers the requirement of higher intake air temperature. Therefore, requirement of higher intake air temperature depends upon the dominating factor between the two opposing factors given above.

Figures 3–5 show the particle size–number distribution for gasoline, ethanol, and methanol at 1200 and 2400 rpm for varying intake air temperatures and λ. It can be observed from Figs. 3–5 that the particle numbers increased as the engine was operated using richer mixtures at each intake air temperature for all test fuels. Peak concentration of particles depends on the mixture strength (i.e., engine load) and intake air temperature (i.e., combustion phasing) for both fuels. It can also be observed from Figs. 3–5 that peak normalized particulate number concentration from gasoline lies between 3.56×10^7–1.75×10^8 particles/cm^3 at 1200 rpm and 5.75×10^7–1.92×10^8 particles/cm^3 at 2400 rpm. The peak normalized number concentration of ethanol lies between 9.99×10^6–1.91×10^8 particles/cm^3 at 1200 rpm and 4.53×10^7–1.57×10^8 particles/cm^3 at 2400 rpm. The peak

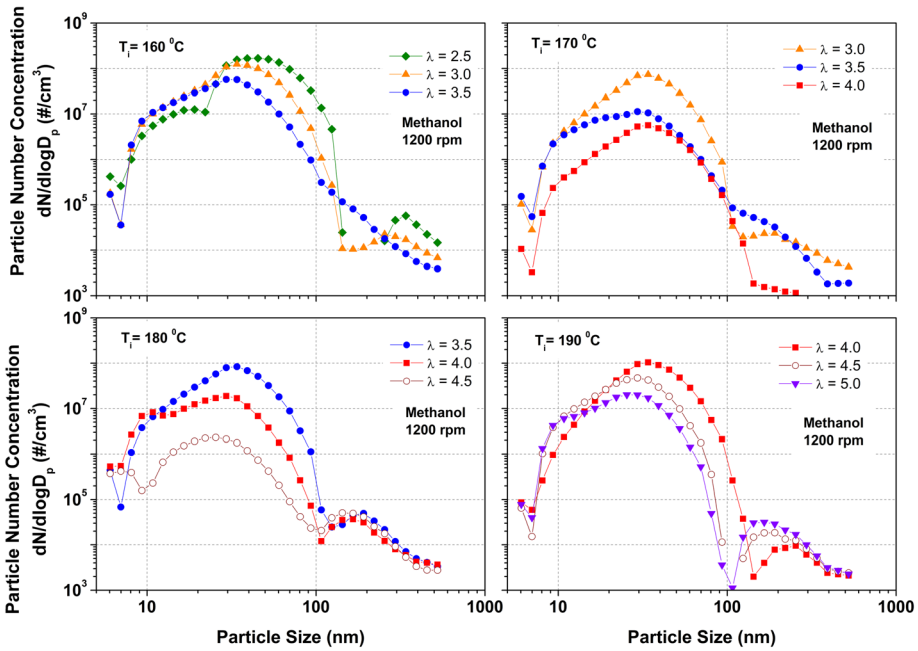

(a) Particle size distribution at 1200 rpm.

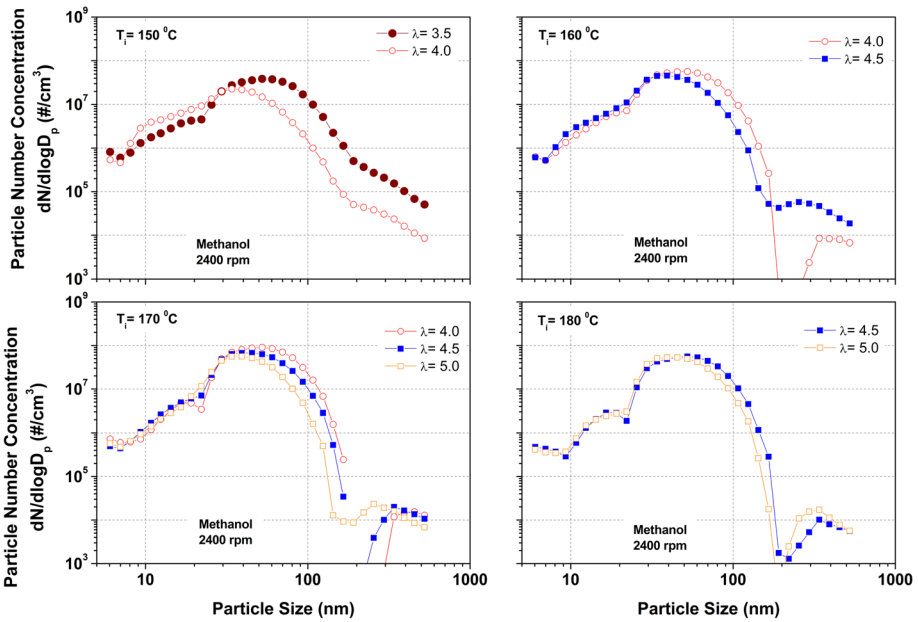

(b) Particle size distribution at 2400 rpm.

Fig. 5 Particle size–number distributions for methanol HCCI combustion with varying intake temperature and λ

normalized number concentration of methanol lies between 2.32×10^6–1.67×10^8 particles/cm^3 at 1200 rpm and 2.29×10^7 –9.04×10^7 particles/cm^3 at 2400 rpm. The maximum normalized peak concentration of particle was lower at higher engine speeds for ethanol and methanol. Methanol showed lower peak normalized number concentration as compared to gasoline and ethanol at both engine speeds. For all test conditions, the particle sizes having significant number of particles were in the range of 6–150 nm.

Price et al. discussed various reasons for non-negligible PM emissions from DI-HCCI gasoline engines [26]. Various factors affecting the PM emissions from HCCI engines explored by Price et al. were piston and wall wetting, charge heterogeneity, condensation, nucleation, ash, and metal emissions. Condensable PM fraction was expected to be significant in HCCI mode for two reasons: First, high unburned gas phase hydrocarbon emissions due to lower combustion temperature in HCCI mode lead to higher particulate phase hydrocarbons, and second, temperature in the expansion stroke is not high enough to oxidize all unburned hydrocarbons that diffuse out of the crevice volume. These hydrocarbons remain in the exhaust and condense, when temperatures become low enough [26].

It can also be observed from these Figs. 3–5 that leaner mixtures have peak particulate concentration for lower mobility diameters at each intake air temperature for all test fuels. It can be noticed from Fig. 4 that mobility diameters for peak particle number concentration using ethanol are in the range of 22–40 nm and 39–60 nm at 1200 and 2400 rpm, respectively. It can also be

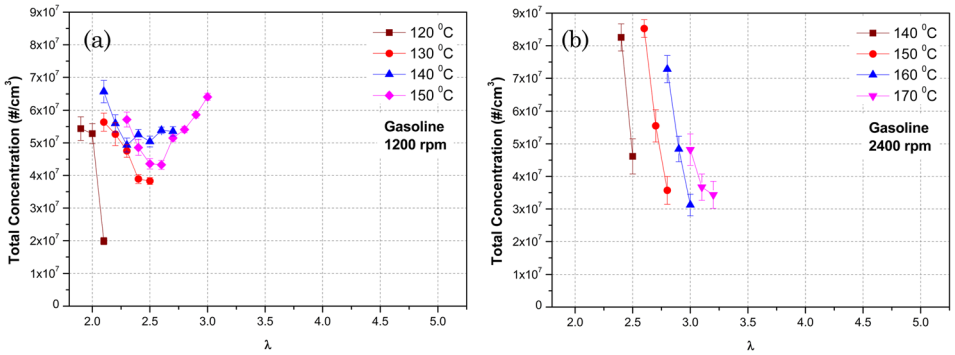

Fig. 6 Variation of total number concentration of particles at (*a*) 1200 rpm (*b*) 2400 rpm for gasoline

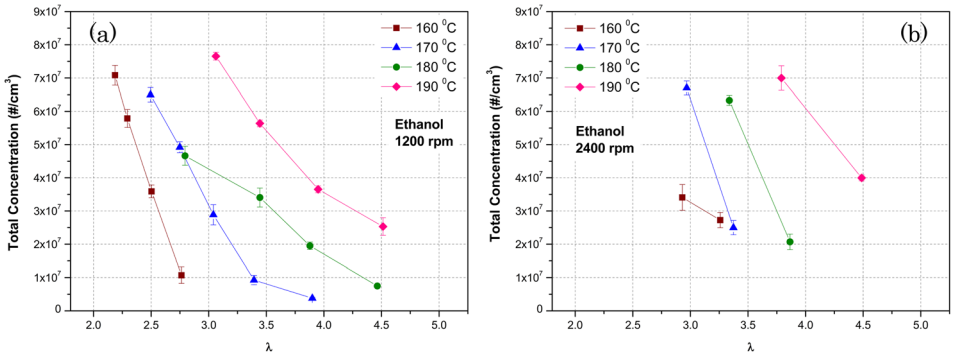

Fig. 7 Variation of total number concentration of particles at (*a*) 1200 rpm (*b*) 2400 rpm for ethanol

noticed from Fig. 5 that mobility diameters for peak particle number concentration using methanol are in the range of 25–45 nm and 34–52 nm at 1200 and 2400 rpm, respectively. Whereas gasoline has mobility diameters corresponding to peak particle number concentration at 1200 and 2400 rpm, respectively, in the size range of 34–80 nm and 34–70 nm. Particles have relatively lower mobility diameters corresponding to the peak number concentration for ethanol and methanol compared to gasoline at 1200 rpm and 2400 rpm. This observation indicates that particles from ethanol and methanol are relatively smaller compared to gasoline. Mobility diameters with peak concentration in gasoline HCCI were larger as compared to gasoline SI engine (< 25 nm) as reported by Gupta et al. [23]. It is also observed that the mobility diameters corresponding to peak concentration of particles become smaller with increasing intake air temperatures.

It can be noticed from Figs. 3–5 that particle size–number distribution curves for gasoline have different behavior in particle size ranging less than 20 nm. Particle number concentration in the size range close to 10 nm has number concentration of the order 10^6 particles/cm^3 for ethanol and methanol, and at lower intake temperatures, some test conditions showed even lower particle concentration (i.e., $<10^6$ particles/cm^3). Gasoline particulates in the size range of 10 nm however have number concentration in the order 10^7 particles/cm^3, which is an order of magnitude higher as compared to ethanol and methanol (Figs. 3–5). On increasing intake air temperature, number of nuclei mode particles increase for all test fuels.

Franklin demonstrated that almost all particles measured in ethanol HCCI combustion with different control strategies are volatile with no measureable concentration of solid accumulation mode particles [30]. In the absence of solid nucleation mode particles, which act as adsorption sites, only gas-to-particle conversion processes are available to the organic vapors in the exhaust, as it is diluted and cooled, leading to homogeneous nucleation and condensation. This leads to the formation of volatile nucleation mode particles. It is also reported that in conventional CI engines, composition of volatile nucleation mode particles, and their characteristics are dominated by lubricating oil with increasing engine loads [34]. This study suggested that higher in-cylinder temperatures lead to formation of higher lubricating oil related nucleation mode particles. The number of particles increases with increasing engine load (richer mixture), due to higher in-cylinder temperature when compared to those with lower engine loads (leaner mixtures) (Figs. 3–5). Sakurai et al. also reported that volatile particulates are composed of at least 95% compounds originating from unburned lubricating oil at light to moderate engine loads in conventional diesel engines [35]. HCCI engines use similar configuration of lubricating system, piston, and piston rings as in conventional CI engines. Therefore, delivery of lubricating oil to the combustion chamber and associated processes in the combustion chamber may also be quite similar [30]. Additionally, THC emissions decrease at higher intake air temperature, while particle numbers increase. It is reported for a hydrogen (SI) engine that with increasing in-cylinder temperature, organic carbon levels of the PM also increase [36]. This was reportedly because of relatively higher breakdown of the lubricating oil film present on the cylinder liner walls. Similar phenomenon may also be taking place in HCCI combustion engines, and upon increasing the intake air temperature, the rate of pressure rise increases rapidly.

Figures 6–8 show the total number concentration of particles at different λ and T_i for gasoline ethanol and methanol at 1200 and 2400 rpm. It is observed from these figures that as the mixture becomes leaner, total particle concentration decreased for all test fuels except two engine operating conditions ($T_i = 140$ and 150 °C for gasoline at 1200 rpm). This suggests that on increasing the

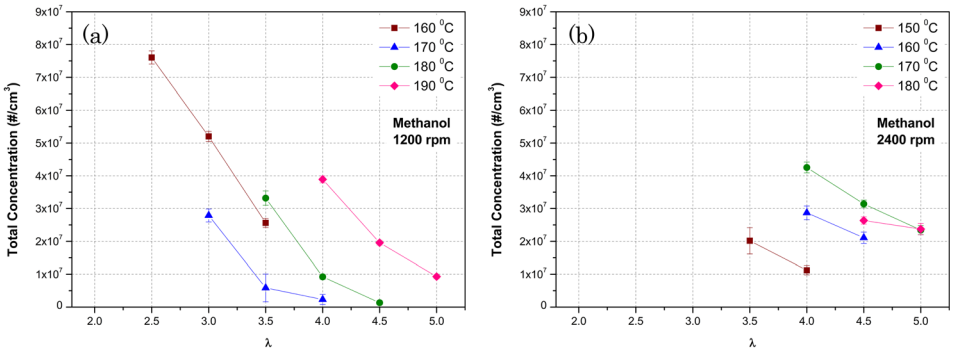

Fig. 8 Variation of total number concentration of particles at (*a*) 1200 rpm (*b*) 2400 rpm for methanol

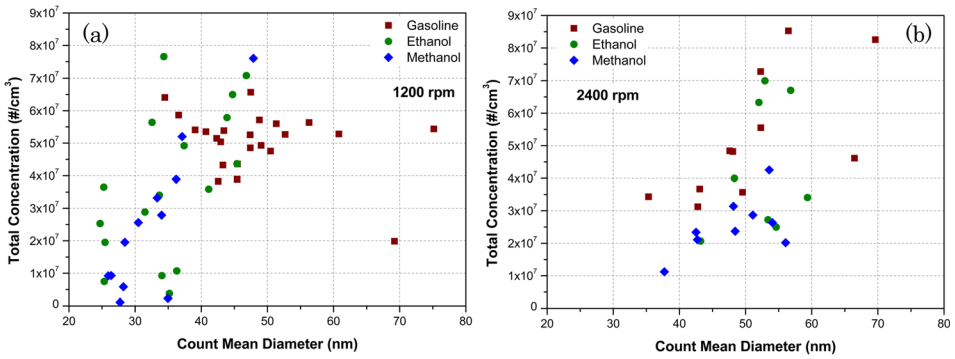

Fig. 9 Variation of total concentration of particles with CMD for gasoline, ethanol, and methanol

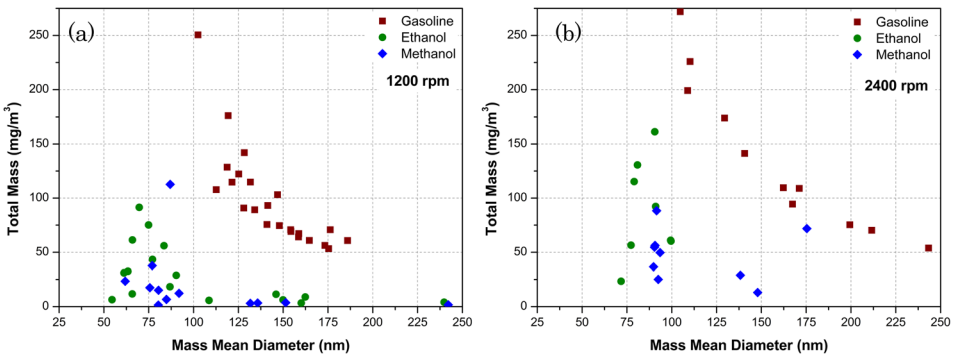

Fig. 10 Variation of total mass of particles with MMD for gasoline, ethanol, and methanol

fueling (load), total particle concentration increases and these trends agree with observations for engines employing conventional combustion modes [23]. Total number concentration of particles increase with increasing intake air temperature for constant fueling, which is possibly due to increase in nuclei mode particles at higher temperature. The maximum number of total particle concentration was lower for methanol as compared to ethanol and gasoline for both engine speeds, except two test points. It can also be concluded from Figs. 6–8 that maximum number concentration of particles increase with increasing engine speeds for gasoline but decreased for ethanol and methanol. The total concentration of particles was in the range of 9.31×10^6–8.53×10^7 particles/cm^3 for all test fuels.

The average particle size can be represented by CMD, which provides a basis for comparing overall size of emitted PM for different engine operating conditions and fuels in HCCI mode. Figure 9 shows the total particle number concentration with respect to calculated CMD of particulates for gasoline, ethanol, and methanol at 1200 and 2400 rpm in HCCI mode. CMD of particulates was in the range of 32–80 nm for gasoline for all test conditions in HCCI mode for both engine speeds. However, CMD of particulates was in the range of 20–50 nm and 35–60 nm for ethanol and methanol under similar test conditions in HCCI. This observation indicated that average diameter of particles emitted from ethanol and methanol were smaller compared to gasoline in HCCI mode. Smaller molecular chain lengths and lower number of carbon–carbon bonds in ethanol and methanol fuel molecules may be responsible for relatively smaller particle diameters. Lower CMD indicated lower concentration of accumulation mode particles and/or higher concentration of nuclei mode particles for

ethanol and methanol in comparison to gasoline. It can be noticed from Fig. 9 that total number concentration of particles is also lower for lower CMD using methanol and ethanol at 1200 rpm.

Figure 10 shows the total particle mass emission with respect to calculated mass mean diameter (MMD) of particulates for gasoline, ethanol, and methanol fuels in HCCI mode at 1200 and 2400 rpm. For all calculations, a constant soot density of 1.0 g/cm^3 was used in this investigation. Schnieder et al. showed that this value of PM density is a reasonable estimate of density for PM originating from engine lubricating oil [37]. This density was also used for PM studies on a gasoline fueled HCCI engine [28]. It can be noticed from Fig. 10 that total mass emission from gasoline is higher as compared to ethanol and methanol at both engine speeds. MMD of particulates was larger as compared to CMD of particulates for all test fuels. MMD for ethanol and methanol were smaller as compared to gasoline. MMD for all test fuels was in the range of 50–200 nm.

4 Conclusions

Experiments were conducted in a HCCI engine operating at different inlet air temperatures and relative air–fuel ratios at 1200 and 2400 rpm using gasoline, ethanol, and methanol to investigate the effect of engine operating conditions on PM emissions. It was found that IMEP was mainly affected by λ in the HCCI mode. HCCI operating region (operating envelope) shrunk with increasing engine speed for all test fuels. Particle numbers increased as engine was operated using richer mixtures at each intake air temperature for all test fuels. The maximum normalized peak concentration of particles was lower at higher engine speeds for ethanol and methanol. Methanol had lower peak normalized number concentration as compared to gasoline and ethanol at both engine speeds. For all test conditions, the particle sizes having significant number of particles were in the range of 6–150 nm. Leaner operating conditions showed peak concentrations for smaller mobility diameters at each intake air temperature for all test fuels. Particles showed smaller mobility diameter corresponding to peak number concentration of ethanol and methanol as compared to gasoline. It was also found that peak concentration of particles shifted toward lower mobility diameter with increasing intake air temperatures. Total particle concentration decreased as engine was operated with leaner mixtures for all test fuels. Total concentration of particles increased with increasing intake air temperature for constant fueling. The total PM number concentration was lower for methanol as compared to ethanol and gasoline. The total concentration of particles was in the range of 9.31×10^6–8.53×10^7 particles/cm^3. CMD and MMD of particles emitted from ethanol and methanol were smaller as compared to gasoline.

Abbreviations

CAD = crank angle degree
CI = compression ignition
CMD = count mean diameter
CO = carbon monoxide
COV = coefficient of variation
DI = direct injection
EEPS = engine exhaust particle sizer
EGR = exhaust gas recirculation
HC = unburned hydrocarbon
HCCI = homogeneous charge compression ignition
IC = internal combustion
IMEP = indicated mean effective pressure
IVC = intake valve closed
IVO = intake valve open
MMD = mass mean diameter
PM = particulate matter
SI = spark ignition
TDC = top dead center
T_i = inlet air temperature
λ = relative air–fuel ratio

References

[1] Shi, L., Cui, Y., Deng, K., Peng, H., and Chen, Y., 2006, "Study of Low Emission Homogeneous Charge Compression Ignition (HCCI) Engine Using Combined Internal and External Exhaust Gas Recirculation (EGR)," Energy, **31**(14), pp. 2665–2676.
[2] Kelly-Zion, P. L., and Dec, J. E., 2000, "A Computational Study of the effect of the Fuel-Type on the Ignition Time in HCCI Engines," Proc. Combust. Inst., **28**(1), pp. 1187–1194.
[3] Li, H., Neill, W. S., and Chippior, W. L., 2012, "An Experimental Investigation of HCCI Combustion Stability Using n-Heptane," ASME J. Energy Resour. Technol., **134**(2), p. 022204.
[4] Mack, J. H., Aceves, S. M., and Dibble, R. W., 2009, "Demonstrating Direct Use of Wet Ethanol in a Homogeneous Charge Compression Ignition (HCCI) Engine," Energy, **34**(6), pp. 782–787.
[5] Maurya, R. K., and Agarwal, A. K., 2009, "Experimental Investigation of the Effect of the Intake Air Temperature and Mixture Quality on the Combustion of a Methanol and Gasoline Fuelled Homogeneous Charge Compression Ignition Engine," Proc. Inst. Mech. Eng., Part D, **223**, pp. 1445–1458.
[6] Maurya, R. K., and Agarwal, A. K., 2011, "Experimental Study of Combustion and Emission Characteristics of Ethanol Fuelled Port Injected Homogeneous Charge Compression Ignition (HCCI) Combustion Engine," Appl. Energy, **88**(4), pp. 1169–1180.
[7] Maurya, R. K., and Agarwal, A. K., 2011, "Effect of Start of Injection on the Particulate Emission From Methanol Fuelled HCCI Engine," SAE Int. J. Fuels Lubr., **4**(2), pp. 204–222.
[8] Tongroon, M., and Zhao, H., 2010, "Combustion Characteristics of CAI Combustion With Alcohol Fuels," SAE Technical Paper No. 2010-01-0843.
[9] Jin, C., Yao, M., Liu, H., Lee, C. F., and Ji, J., 2011, "Progress in the Production and Application of n-Butanol as a Biofuel," Renewable Sustainable Energy Rev., **15**(8), pp. 4080–4106.
[10] Hansen, A. C., Kyritsis, D. C., and Lee, C. F., "Characteristics of Biofuels and Renewable Fuel Standards," in *Biomass to Biofuels—Strategies for Global Industries*, A. A. Vertes, H. P. Blaschek, H. Yukawa, and N. Qureshi, eds., Wiley, NY.
[11] Gao, T., Divekar, P., Asad, U., Han, X., Reader, G. T., Wang, M., Zheng, M., and Tjong, J., 2013, "An Enabling Study of Low Temperature Combustion With Ethanol in a Diesel Engine," ASME J. Energy Resour. Technol., **135**(4), p. 042203.
[12] Hansen, A. C., Zhang, Q., and Lyne, P. W. L., 2005, "Ethanol–Diesel Fuel Blends–A Review," Bioresour. Technol., **96**(3), pp. 277–285.
[13] Christie, M., Fortino, N., and Yilmaz, H., 2009, "Parameter Optimization of a Turbo Charged Direct Injection Flex Fuel SI Engine," SAE Int. J. Engines, **2**(1), pp. 123–133.
[14] Sjoberg, M., and Dec, J., 2010, "Ethanol Autoignition Characteristics and HCCI Performance for Wide Ranges of Engine Speed, Load and Boost," SAE Int. J. Engines, **3**(1), pp. 84–106.
[15] Martinez-Frias, J., Aceves, S. M., and Flowers, D. L., 2007, "Improving Ethanol Life Cycle Energy Efficiency by Direct Utilization of Wet Ethanol in HCCI Engines," ASME J. Energy Resour. Technol., **129**(4), pp. 332–337.
[16] Khaliq, A., and Trivedi, S. K., 2012, "Second Law Assessment of a Wet Ethanol Fuelled HCCI Engine Combined With Organic Rankine Cycle," ASME J. Energy Resour. Technol., **134**(2), p. 022201.
[17] Viggiano, A., and Magi, V. A., 2012, "Comprehensive Investigation on the Emissions of Ethanol HCCI Engines," Appl. Energy, **93**, pp. 277–287.
[18] Petrovic, V. S., Jankovic, S. P., Tomic, M. V., Jovanovic, Z. S., and Knežević, D. M., 2011, "The Possibilities for Measurement and Characterization of Diesel Engine Fine Particles–A Review," Therm. Sci., **15**(4), pp. 915–938.
[19] Dorie, L. D., Bagley, S. T., Leddy, D. G., and Johnson, J. H., 1987, "Characterization of Mutagenic Subfractions of Diesel Exhaust Modified by Ceramic Particulate Traps," Environ. Sci. Technol., **21**(8), pp. 757–765.
[20] Kayes, D., Liu, H., and Hochgreb, S., 1999, "Particulate Matter Emission During Start-up and Transient Operation of a Spark-Ignition Engine," SAE Technical Paper No. 1999-01-3529.
[21] Maricq, M. M., Podsiadlik, D. H., and Chase, R. E., 1999, "Examination of the Size-Resolved and Transient Nature of Motor Vehicle Particle Emissions," Environ. Sci. Technol., **33**(10), pp. 1618–1626.
[22] Maricq, M. M., Podsiadlik, D. H., and Chase, R. E., 1999, "Gasoline, Vehicle Particle Size Distributions: Comparison of Steady State, FTP, and USO6 Measurements," Environ. Sci. Technol., **33**(12), pp. 2007–2015.
[23] Gupta, T., Kothari, A., Srivastava, D. K., and Agarwal, A. K., 2010, "Measurement of Number and Size Distribution of Particles Emitted From a Mid-Sized Transportation Multipoint Port Fuel Injection Gasoline Engine," Fuel, **89**(9), pp. 2230–2233.
[24] Epping, K., Aceves, S. M., Bechtold, R., and Dec, J., 2002, "The Potential of HCCI Combustion for High Efficiency and Low Emissions," SAE Technical Paper No. 2002-01-1923.
[25] Kaiser, E. W., Yang, J., Culp, T., and Maricq, M. M., 2002, "Homogeneous Charge Compression Ignition Engine-Out Emissions—Does Flame Propagation Occur in Homogeneous Charge Compression Ignition?," Int. J. Engine Res., **3**(4), pp. 185–195.
[26] Price, P., Stone, R., Misztal, J., Xu, H., Wyszynski, M., and Wilson, T., 2007, "Particulate Emissions From a Gasoline Homogeneous Charge Compression Ignition Engine," SAE Technical Paper No. 2007-01-0209.

[27] Misztal, J., Xu, H., Tsolakis, A., Wyszynski, M. L., Constandinides, G., Price, P., and Qiao, J., 2009, "Influence of Inlet Air Temperature on Gasoline HCCI Particulate Emissions," Combust. Sci. Technol., **181**(5), pp. 695–709.
[28] Misztal, J., Xu, H. M., Wyszynski, M. L., Price, P., Stone, R., and Qiao, J., 2009, "Effect of Injection Timing on Gasoline Homogeneous Charge Compression Ignition Particulate Emissions," Int. J. Engine Res., **10**(6), pp. 419–430.
[29] Maurya, R. K., Srivastava, D. K., and Agarwal, A. K., 2011, "Experimental Investigations of Particulate Emitted by an Alcohol-Fuelled HCCI/CAI Combustion Engine," Int. Energy J., **12**(1), pp. 29–38.
[30] Franklin, L., 2010, "Effects of Homogeneous Charge Compression Ignition (HCCI) Control Strategies on Particulate Emissions of Ethanol Fuel," Ph.D. thesis, University of Minnesota, ProQuest, UMI Dissertation, Minneapolis, MN.
[31] Singh, A. P., Lukose, J., Gupta, T., and Agarwal, A. K., 2013, "Characterization of Exhaust Particulates from Diesel Fuelled Homogenous Charge Compression Ignition Combustion Engine," J. Aerosol Sci., **58**, pp. 71–85.
[32] Johansson, T., Borgqvist, P., Johansson, B., Tunestål, P., and Aulin, H., 2010, "HCCI Heat Release Data for Combustion Simulation, based on Results from a Turbocharged Multi Cylinder Engine," SAE Paper No. 2010-01-1490.
[33] Johansson, T., Johansson, B., Tunestål, P., and Aulin, H., 2009, "HCCI Operating Range in a Turbo-charged Multi Cylinder Engine With VVT and Spray-Guided DI," SAE Paper No. 2009-01-0494.
[34] Tobias, H. J., Beving, D. E., Ziemann, P. J., Sakurai, H., Zuk, M., McMurry, P. H., Zarling, D., Waytulonis, R., and Kittelson, D. B., 2001, "Chemical Analysis of Diesel Engine Nanoparticles Using a Nano-DMA-Thermal Desorption Particle Beam Mass Spectrometer," Environ. Sci. Technol., **35**(11), pp. 2233–2243.
[35] Sakurai, H., Tobias, H. J., Park, K., Zarling, D., Docherty, K. S., Kittelson, D. B., McMurry, P. H., and Ziemann, P. J., 2003, "On-Line Measurements of Diesel Nanoparticle Composition and Volatility," Atmos. Environ., **37**(9–10), pp. 1199–1210.
[36] Miller, A. L., Stipe, C. B., Habjan, M. C., and Ahlstrand, G. G., 2007, "Role of Lubrication Oil in Particulate Emissions From a Hydrogen-Powered Internal Combustion Engine," Environ. Sci. Technol., **41**(19), pp. 6828–6835.
[37] Schneider, J., Hock, N., Weimer, S., and Borrmann, S., 2005, "Nucleation Particles in Diesel Exhaust: Composition Inferred From in Situ Mass Spectrometric Analysis," Environ. Sci. Technol., **39**(16), pp. 6153–6161.